

Development of Poly(imide-*b*-amic acid) Multiblock Copolymer Thin Film

Keisuke Kuriyama,[†] Shigeo Shimizu,[‡] Kazuhiro Eguchi,[‡] and Thomas P. Russell^{*,†}

Department of Polymer Science and Engineering, University of Massachusetts, Amherst, Massachusetts 01003, and Display Laboratories, JSR Corporation, Yokkaichi, Mie 510-8552, Japan

Received January 3, 2003; Revised Manuscript Received April 21, 2003

ABSTRACT: The preparation of poly(imide-*b*-amic acid) multiblock copolymers was examined by blending solutions of soluble end-functionalized polyimide and polyamic acid homopolymers. The terminal end groups of the soluble polyimide (PI) and poly(amic acid) (PAA) can react to form a multiblock PI/PAA copolymer that was, subsequently, fully imidized. Atomic force microscopy (AFM) height images showed that surface topography of thin solution-cast films of PI/PAA blends depended strongly on the aging time of the solution. Macroscopically phase-separated structures were seen with short aging times, whereas uniform flat surfaces were seen with increasing aging time. For comparison, mixtures of end-capped PI/PAA (nonreactive) were also prepared that showed macrophase-separated surface structures irrespective of the aging time of the solution. Static light scattering measurements showed an increase in the average molecular weight of the end-functionalized blend of PI/PAA, suggesting the formation of poly(imide-*b*-amic acid) multiblock copolymers. AFM images in the phase mode and X-ray photoelectron spectroscopy showed that the phase-separated morphology had a much higher surface composition of PI than the blend ratio.

Introduction

Recent progress has made it possible to develop a new class of polyimides (PIs) that are soluble in the polar organic solvents.^{1–3} Solvent-soluble polyimides have a wide variety of applications in microelectronics, since thin PI films with excellent thermal and chemical stability, low dielectric constant, and enhanced mechanical properties can be easily prepared at relatively low temperatures (around 80 °C).^{4–6} Solvent-soluble PIs, however, exhibit lower adhesion to the substrate and poorer wear resistance, since these polymers do not order like other polyimides. This inability to order arises from the introduction of flexible moieties or bulky substitutes into the rigid chemical structure of PI. These substituents hinder intersegmental packing and, therefore, enhance solubility. Poly(amic acid) (PAA), on the other hand, is soluble due to its flexibility and polarity and can be converted to PI thermally. Although PAA shows excellent adhesion to the substrate as well as durability, it requires a relatively high temperature (200 °C) for extended periods of time to be fully cyclized to the corresponding PI.

Poly(imide-*b*-amic acid) (P(I-*b*-AA)) multiblock copolymers, therefore, represent a route to enhance the solubility of PI and to impart unique properties to the resultant film. In contrast to the conventional modification of PI materials using blends of PAAs, where intermolecular exchange (transamidization) reactions will occur to form homogeneous random copolymers, P(I-*b*-AA) multiblock copolymers have blocks consisting of each component. Consequently, P(I-*b*-AA) multiblock copolymers are expected to show novel properties based on the microphase-separated structure.

Here, the preparation of P(I-*b*-AA) multiblock copolymer thin films as a novel polyimide material was

examined by solution mixing PI and PAA. In principle, solvent-soluble PI can react with PAA via reactive end groups, since solvent-soluble PI is prepared by chemical imidization of a precursor PAA. The reactive end groups are preserved through the polycondensation reaction. By adding a solution of PAA into a PI solution, reaction will occur forming multiblock copolymers. The blend solutions of PI and PAA (PI/PAA) at various blend ratios were prepared. The surface topography of thin cast films was investigated by atomic force microscopy (AFM). For comparison, blend solutions of end-capped, nonreactive PI/PAA were prepared. Differences in the surface topography in the two cases (along with static light scattering measurements) clearly indicated the formation of multiblock copolymers.

Experimental Section

Preparation of PI and PAA. Figure 1 shows the chemical structures of the PI and PAA used in this study. The precursor PAA of the solvent-soluble PI was prepared by polycondensation between the dianhydride of 1,3,3a,4,5,9b-hexahydro-8-methyl-5-(tetrahydrofuran-2-yl)naphtho[1,2-*c*]furan-1,3-dione (MTDA) and the diamine of 4,4'-diamino-2,2'-bis(trifluoromethyl)biphenyl (TFMB). MTDA has a bulky structure that hinders the strong intermolecular interactions, which render it soluble in an organic solvent. The fluorine atoms in TFMB serve as a label that can be easily detected by X-ray photoelectron spectroscopy (XPS). Polycondensation was carried out by adding MTDA powder into a γ -butyrolactone (γ -BL) solution of TFMB with continuous mechanical stirring at room temperature for several hours. The molar amount of MTDA was larger than that of TFMB so that the resultant precursor PAA has MTDA end groups. Successive chemical imidization was conducted by adding pyridine and acetic acid anhydride (several times the molar quantity of the diamine) to the solution at 80 °C. After the reaction, excess pyridine and acetic acid were removed by distillation under reduced pressure. PAA for another blend component was prepared by the polycondensation of MTDA and *p*-phenylenediamine (PDA) in γ -BL. The molar amount of PDA was adjusted to be greater than MTDA so that the resultant PAA has end groups of PDA.

[†] University of Massachusetts.

[‡] JSR Corporation.

* Author to whom correspondence should be addressed.

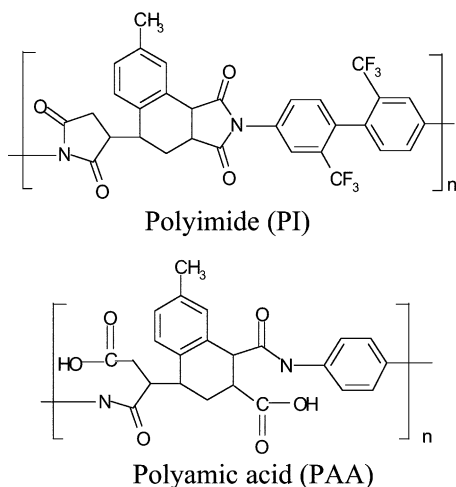


Figure 1. Chemical structures of PI and PAA used in this study for the blend components.

Combination of PAA with amine end groups and PI with anhydride end groups is expected to react to form a multiblock copolymer.

End-Capping of PI. For comparison, end-capped PI that cannot react with PAA was also prepared. To prevent the condensation reaction with amine end groups of PAA, anhydride end groups of PI were terminated by adding monoamine reagent. Excess amounts of aniline or 4-trifluoromethylaniline were added into the PI solution. After stirring for 18 h at room temperature, pyridine and acetic acid anhydride were added to imidize the amic acid caused by condensation between anhydride end group and monoamine molecule. The solution was stirred at 80 °C for more than 5 h. The solution was then poured into a methanol bath to precipitate the polymer. The precipitate was filtered using a glass filter and washed several times with methanol and dried. The resultant white powder was further dried in the vacuum oven at 30 °C for several hours. For the PI powder treated with 4-trifluoromethylaniline, the introduction of a 4-trifluoromethyl substituent into the polymer molecule was easily confirmed as a new peak in the ^{19}F NMR spectrum of polymer dissolved in $d\text{-DMSO}$ (dimethyl sulfoxide).

Preparation of Blend Solution. Blend solutions of various blend ratios (wt %) were prepared by solution blending PI and PAA in $\gamma\text{-BL}$. The concentration of blend solution was 3 wt %. The solutions were stored in a refrigerator (~ 5 °C) to avoid decomposition of PAA.

Film Preparation on the Substrate. The blend solution was spin-coated at 1700 rpm onto a clean Si wafer with a 2 nm native oxide layer. The Si wafer was precleaned by immersion into the sulfuric acid with NOCHROMIX to remove organic contaminants on the surface. The thin films of the blends were prebaked at 80 °C for 20 min on a hot plate. Some samples were subsequently postbaked at 200 °C for 90 min. The film thickness of all samples were about 50 nm based on optical ellipsometry measurements.

Atomic Force Microscopy (AFM). AFM imaging of the blend films on the substrate was performed using a Digital Instruments Nanoscope IIIa SPM controller. Topographic and phase images were obtained simultaneously in the tapping mode. Phase images were used to map the surface morphology since only the PI component contains fluorine.

Static Light Scattering Measurement. The average molecular weights of polymers were evaluated by static light scattering measurements of dilute solutions in $\gamma\text{-BL}$. Static light scattering measurements were carried out using a ALV-5000 light scattering system. Measurements of the excess Rayleigh factor R_θ at various scattering angles ($30^\circ < \theta < 100^\circ$) were made for 5–6 concentrations ($1 \text{ mg/mL} < C < 10 \text{ mg/mL}$) at 15 °C. An average of nine measurements was used, since the scattered light intensity was quite low. The weight-average molecular weight M_w , second virial coefficient A_2 , and

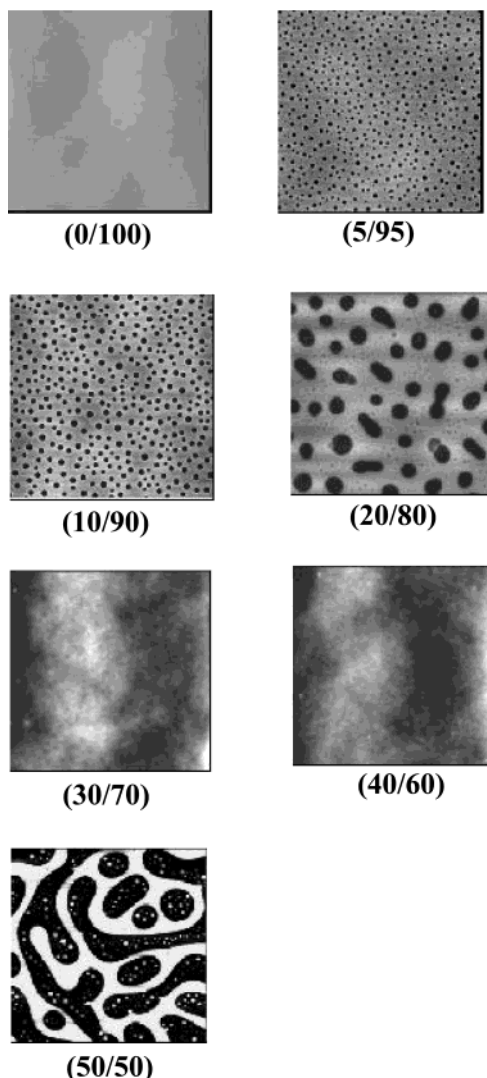


Figure 2. AFM height images of PI/PAA blend thin films with various blend ratios. The blend films were prepared from blend solutions aged 1 day after blending. Scan areas are $40 \mu\text{m} \times 40 \mu\text{m}$ for all cases, and the brighter portion describes a higher portion on the surface. Full height scale is 20 nm.

the root-mean-squared z -average radius of gyration $\langle s^2 \rangle_z$ were then determined from the Zimm equation:

$$\begin{aligned} \frac{Kc}{R\theta} &= \frac{1}{M_w} \left(1 + \frac{16\pi^2}{3\lambda^2} \langle s^2 \rangle_z \sin^2 \frac{\theta}{2} \right) + 2A_2c \\ &= \frac{1}{M_w} \left(1 + \frac{\langle s^2 \rangle_z}{3n^2} q^2 \right) + 2A_2C \end{aligned}$$

where

$$K = \frac{4\pi n^2}{\lambda^4 N_A} \left(\frac{dn}{dc} \right)^2 \quad q = \frac{4\pi n}{\lambda} \sin \frac{\theta}{2}$$

n is the refractive index of the solvent, λ is the wavelength of the incident light (514 nm), and N_A is Avogadro's number. Measured R_θ at a set of c and q were plotted on a single grid (Zimm plot). The linear plots obtained confirmed the absence of an anomalous polyelectrolyte effect of PAA, which can often be observed in N -methylpyrrolidinone solutions and that can prevent accurate evaluation of the molecular weight.^{7,8}

The differential refractive index increment (dn/dc) was measured using a differential refractive index photometer RM-102 (Otsuka Electronics Co. Ltd.) at a temperature of 15 °C.

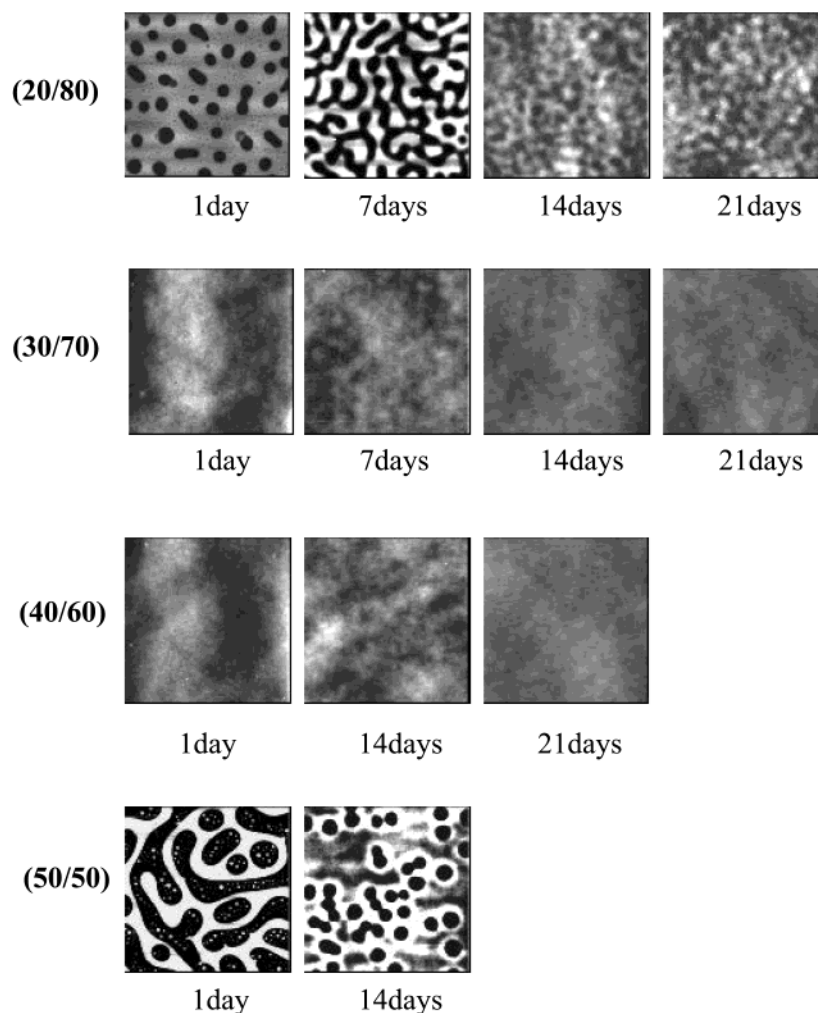


Figure 3. AFM height images of various blend films prepared from solutions aged different time after blending. Scan areas are $40\ \mu\text{m} \times 40\ \mu\text{m}$ for all cases, and the brighter portion describes the higher portion on the surface. Full height scale is 20 nm.

More than five concentrations ($1\ \text{mg/mL} < C < 5\ \text{mg/mL}$) of γ -BL solutions were measured.

XPS Measurement. Surface chemical compositions of the homopolymer films and their blends were measured by XPS using a Physical Electronics Inc. model 5100 with monochromated Al K α (1486.6 eV) X-rays operated at 400 W at takeoff angles of 15° and 75° . The postbaked thin films prepared on the Si wafer were dried in a vacuum oven for 24 h to remove residual solvent. Since only the PI component has fluorine atoms, the integrated signal intensity ratio of F/N was used for calculation of surface composition of the blend film.

Results and Discussion

AFM Observation of PI/PAA Blend Spin-Coated Films. Figure 2 shows AFM height images of PI/PAA blend thin films with various blend ratios. The films were prepared from solutions of the mixtures that were aged for 1 day prior to casting. As expected, the PAA homopolymer films are smooth and featureless. For films of the 5/95:PI/PAA mixture, depressions having a uniform diameter of $\sim 500\ \text{nm}$ were observed. With increasing PAA concentration the lateral size of the depressions increased. The nonuniformity of the films indicates that PAA and PI are phase separating in these thin films and that one component dewets the other. Such behavior has been previously seen for numerous thin film mixtures of incompatible polymers.^{9,11} However, for films of the 30/70 and 40/60 PI/PAA mixtures, the surface is found to be featureless and smooth. With

a further increase in the PAA concentration, as shown for the 50/50 mixtures, a phase-separated structure is again observed, but the height of the depressions is much greater than that seen for the lower PAA concentrations. The concentration dependence of the morphology in the PI/PAA films is quite different than that seen for most other thin film mixtures, where, typically, a systematic change in the morphology of the thin films is observed.

Figure 3 shows a series of AFM images obtained on thin films having different PI/PAA compositions as a function of the time allowed for PI and PAA to mix in the γ -BL. For the 20/80 mixtures, pronounced variations in the surface topography are evident. However, as aging times of the mixtures in solutions are increased, the average variation in the height decreases, indicating that the polymers undergo a change while mixing in the γ -BL. For the 30/70 and 40/60 mixtures, the thin films were smooth in all cases, regardless of the solution aging time. However, for the 50/50 mixture, a strongly phase-separated morphology was observed initially. With increasing aging time of the solution, the average size of the surface features is seen to decrease. Taken together, these data indicate that the PAA and PI are changing with the aging time of the solution and that the rate of change depends on the concentration of the mixtures.

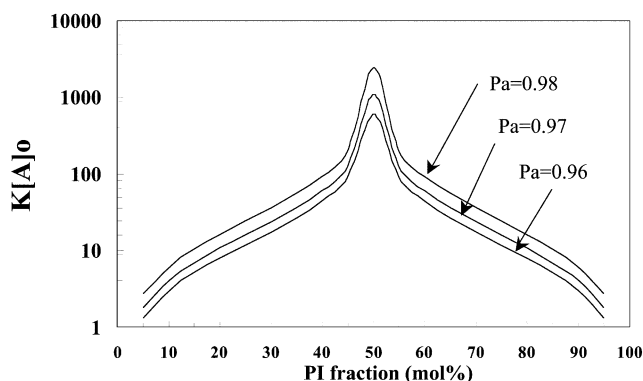


Figure 4. Relationship between $K[A]_0$ and molar ratio of PI (as a monomer) as a function of the extent of reaction (P_a). The $K[A]_0$ value was calculated based on eq 3. The $K[A]_0$ value increases rapidly when the molar ratio approaches 50/50, corresponding to the stoichiometric composition.

Since the condensation of the anhydride and diamine to the amic acid is an equilibrium reaction, then chemical equilibration of the condensation with non-stoichiometric concentrations must be considered.^{12–14} If two types (A,B) of mutually reacting functional groups are involved in the condensation reaction, the equilibrium constant, K , can be written by using the concentrations of reagents and products as

$$K = \frac{[-AB-]}{[A][B]} = \frac{p_A[A]_0}{(1-p_A)(1-p_B)[A]_0[B]_0} \quad (1)$$

where $[A]_0$, $[B]_0$, p_A , and p_B describe initial concentrations of A and B and the extent of reaction conversion of each group, respectively. If the molar ratio $r = [A]_0/[B]_0$ is taken as the parameter defining the stoichiometry of the initial system, then

$$rp_A = p_B \quad (2)$$

and eq 1 can be rewritten as

$$K = \frac{rp_A}{(1-p_A)(1-rp_A)[A]_0} \quad (3)$$

From this equation, the relationship between $K[A]_0$ and molar ratio can be obtained. In Figure 4, the relationship between $K[A]_0$ and PI concentration is shown. The $K[A]_0$ value increases rapidly when the PI fraction approaches 50/50, the balanced stoichiometric composition. This indicates that chemical equilibrium can be reached rapidly near the stoichiometric blend composition.

The relationship between the time-dependent surface topography and blend ratio (w/w) as shown in Figure 3, therefore, can simply be explained in terms of the concentration dependence of the reaction rate. The time-independent smooth surfaces observed for the 30/70 and 40/60 mixtures may be ascribed to the faster reaction rate of the PI and PAA in solution rather than a miscibility window. The blend ratios in the vicinity of maximum point of reaction rate are noteworthy for practical applications.

Surface Morphology of PI/PAA Blend Thin Film Using End-Capped PI. For comparison, PI, end-capped with aniline and 4-trifluoroaniline, was prepared, and the surface topographies of blends consisting of end-capped PI and PAA were examined. Figure 5 shows

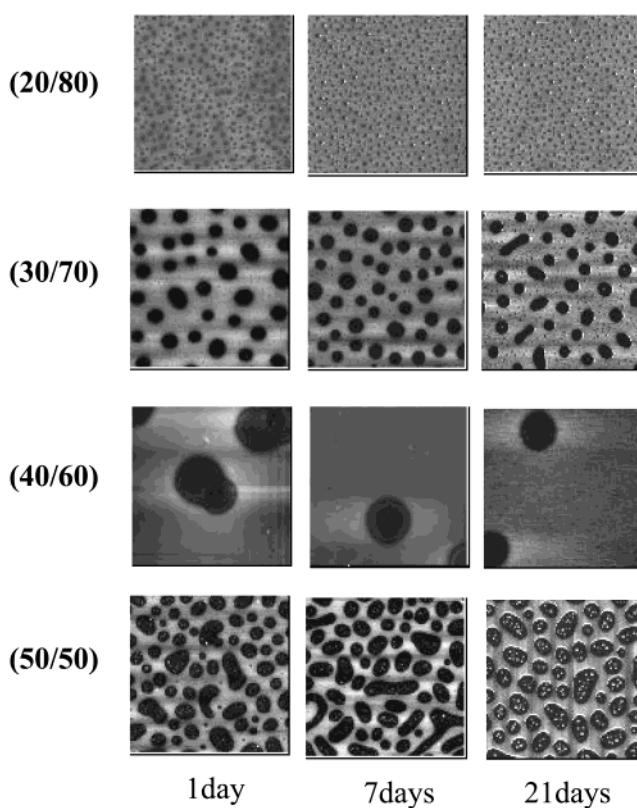


Figure 5. AFM height images of various blend films prepared from aniline-capped PI/PAA blend solutions aged different times after blending. Scan areas are $40 \mu\text{m} \times 40 \mu\text{m}$ for all cases. Full height scale is 20 nm.

AFM height images of films prepared from blends of aniline-capped PI and PAA solutions aged for different times after mixing. It is apparent from Figure 5 that the surface topography of aniline-capped PI/PAA thin films strongly depends on the blend ratio, and phase separation is observed for all compositions. Furthermore, the surface topographies did not depend on the solution aging time even for times up to 3 weeks. Thus, stable phase-separated films could be achieved by using the combination of aniline-capped PI/PAA. In addition, the surface topography of 4-trifluoromethylaniline-capped PI/PAA blend films (shown in Figure 6) displayed topographies similar to the aniline-capped PI/PAA blend films. No change in topography could be detected even after 3 months of solution aging. Comparison of Figures 5 and 6 with Figure 3 thus confirms the argument that the non-end-capped PI/PAA blends react in solution despite the long-chain nature of the polymers, producing P(I-*b*-AA) multiblock copolymers.

Characterization of Polymer Solutions Using Static Light Scattering Measurements. Zimm plots for non-end-capped PI/PAA blend solutions are shown in Figure 7 for blend ratios of 10/90, 30/70, and 40/60 after a solution aging time of 3 weeks. All the mixtures yielded linear plots indicating the absence of anomalous polyelectrolyte effects of PAA, thereby ensuring an accurate determination of the molecular weight. Table 1 shows the parameters determined from the static light scattering measurements. The weight-average molecular weights of the polymers in the blend solutions were greater than the sum of the molecular weights of each component for all blend ratios, though the molecular weight distribution may have changed. These data clearly indicate that intermolecular reactions have

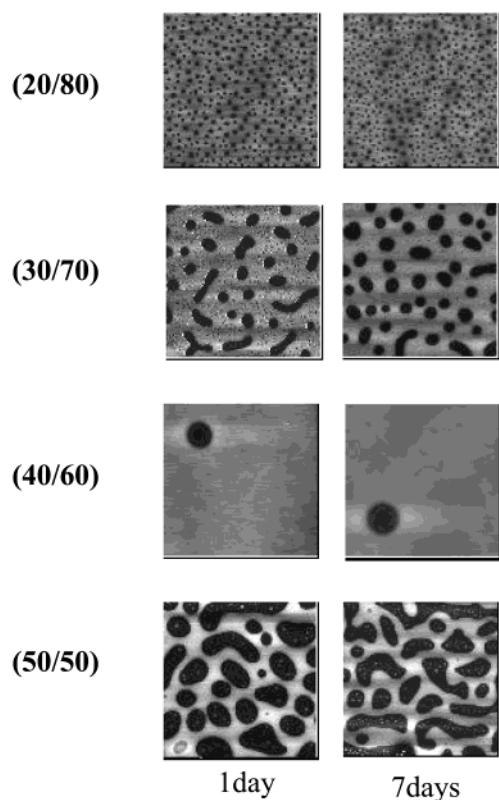


Figure 6. AFM height images of various blend films prepared from 4-trifluoromethylaniline-capped PI/PAA blend solutions aged different time after blending. Scan areas are $40\ \mu\text{m} \times 40\ \mu\text{m}$ for all cases. Full height scale is 20 nm.

occurred, giving rise to the formation of multiblock copolymers. The average molecular weight, however, is rather low, though, even in the case of (PI/PAA) = 40/60, where the average stoichiometric ratio should be close to unity. This suggests a decomposition of PAA to the corresponding dianhydride and diamine monomer followed by a redistribution of these molecules in the formation of multiblock copolymers at equilibrium.¹⁶ In light of the measured average molecular weights of component PI and PAA, PI molecules having PAA fragments on both ends would be the most probable P(I-*b*-AA) multiblock copolymer formed.

Detailed Surface Phase Separation of P(I-*b*-AA) Block Copolymers. The PI and PAA block components were seen to be immiscible by the phase separation behavior of the end-capped PI/PAA mixtures. It was also seen that P(I-*b*-AA) multiblock copolymers, with PI fractions of 30 and 40 wt %, showed a uniform, flat surface over macroscopic distances ($40\ \mu\text{m} \times 40\ \mu\text{m}$), as shown in Figure 3. A detailed AFM study was performed to gain more information on the morphology of the films. AFM phase images were obtained simultaneously with the height images, since only the PI component has fluorine atoms that may alter the specific interaction with the scanning tip.

Figure 8 shows AFM height (top) and phase images (bottom) of P(I-*b*-AA) multiblock copolymer with 40 wt % PI. Line scans across the films are also shown. A patchy pattern with small height variations was found with corresponding differences in the phase images. A comparison of the height and phase images suggests that each portion has a distinct chemical composition difference. This may result from a microphase separation. More than likely, these data show the presence of PI or PAA homopolymers.

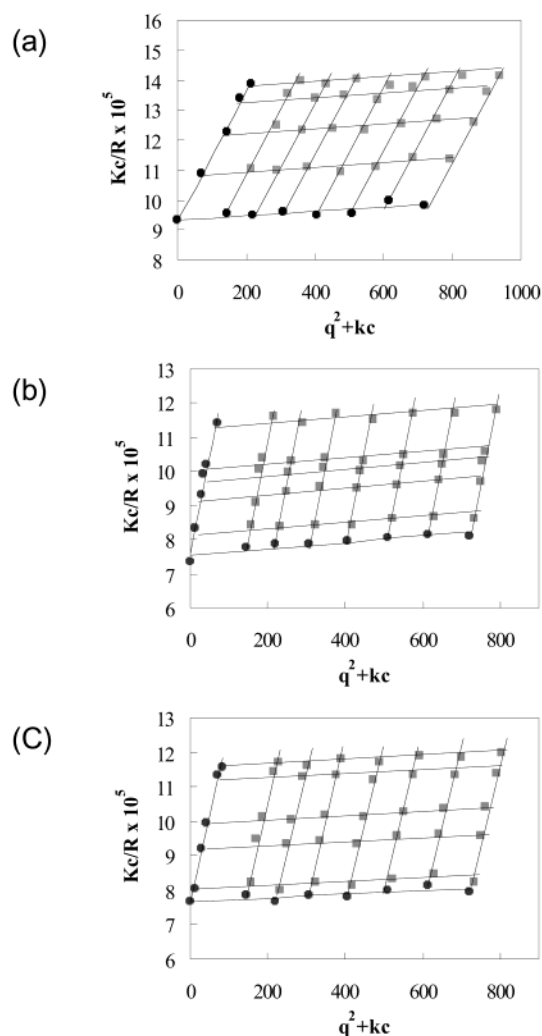


Figure 7. Zimm plots for non-end-capped PI/PAA blend solutions. The blend ratios are (a) (PI/PAA = 10/90), (b) (PI/PAA = 30/70), and (c) (PI/PAA = 40/60), respectively. Aging time is 3 weeks.

Table 1. Molecular Parameters Determined by Static Light Scattering Measurement^a

sample	M_w (g/mol)	$10^4 A_2$ (mL mol/g ²)	R_g (nm)	dn/dc (mL/g)
polyimide (PI)	5 500	28.6	8.3	0.237
polyamic acid (PAA)	6 900	15.3	9.2	0.205
PI/PAA = 10/90	10 700	38.5	21.5	0.188
PI/PAA = 30/70	13 200	20.6	27.2	0.177
PI/PAA = 40/60	13 000	17.5	20.1	0.173

^a M_w , A_2 , and R_g are weight-average molecular weight, second virial coefficient, and z -average radius of gyration, respectively.

Figure 9 shows AFM height (top) and phase images (bottom) of P(I-*b*-AA) multiblock copolymer with a 30 wt % PI fraction. Images similar to the 40% material are seen, though the height and phase images are inverted in comparison to Figure 8. This indicates that the chemical composition of the multiblock copolymers segregated to the surface depends on the blend ratio. This opens the possibility of controlling the extent of surface segregation of the components. The phase images of multiblock copolymers at lower magnification ($5\ \mu\text{m} \times 5\ \mu\text{m}$), shown in Figure 10, confirm this. Such surface phase-separated structure is characteristic of multiblock copolymers, as opposed to a random copolymer.

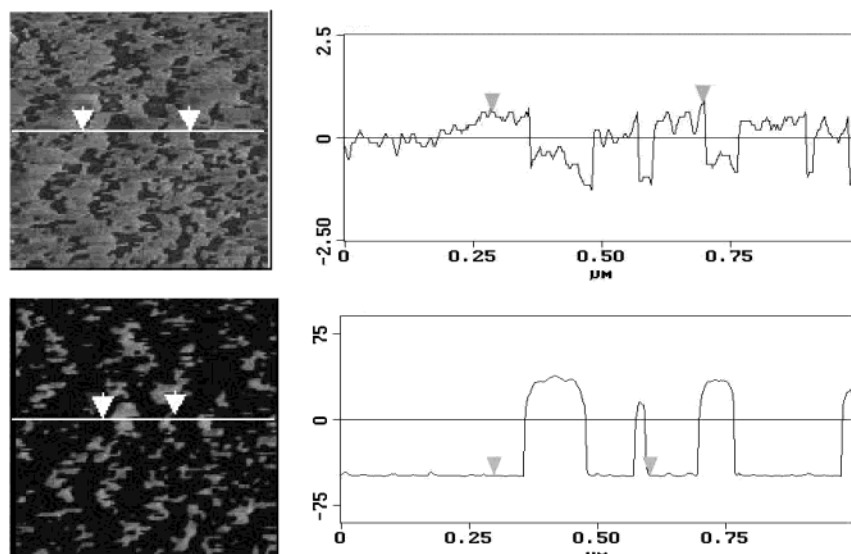


Figure 8. AFM height (above) and phase image (below) of P(I-*b*-AA) multiblock copolymer with PI component of 40 wt %. Scan area is $2\ \mu\text{m} \times 2\ \mu\text{m}$. Cross-sectional profiles at indicated lines near the center of figures are also presented. Full scale of height image is 5 nm, and that of phase image is 160° .

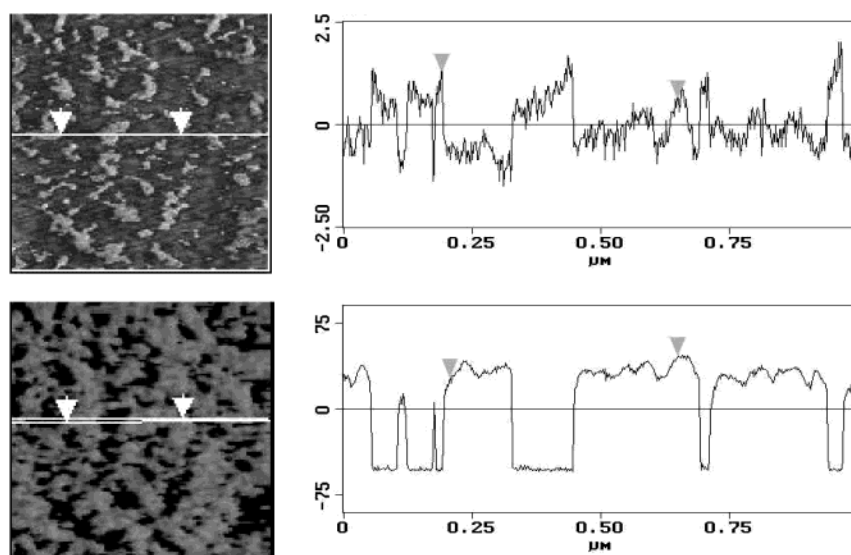


Figure 9. AFM height (above) and phase image (below) of P(I-*b*-AA) multiblock copolymer with PI component of 30 wt %. Scan area is $2\ \mu\text{m} \times 2\ \mu\text{m}$. Full scale of height image is 5 nm, and that of phase image is 160° .

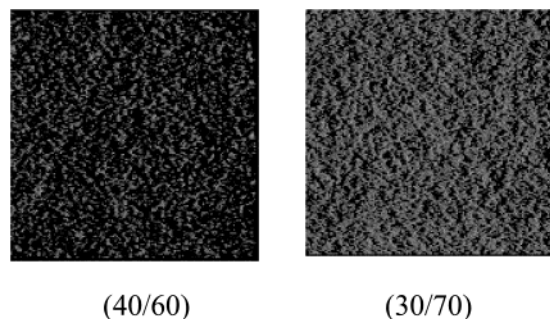


Figure 10. Comparison of phase images of multiblock copolymers with different PI composition. Scan area is $5\ \mu\text{m} \times 5\ \mu\text{m}$ and full scale is 160° .

Surface Chemical Analysis of P(I-*b*-AA) Multiblock Copolymers. Table 2 shows the surface compositions of PI/PAA blend films as measured by XPS. The PI composition was calculated by dividing the integrated signal ratio of F/N of the blend films by that of the homopolymer PI film, since only the PI component has

Table 2. Surface PI Compositions for PI/PAA Blend Films Revealed by the XPS Measurements^a

PI/PAA blend ratio (w/w)	100/0	30/70	40/60
surface PI composition (%)	100	94.8	126.7

^a PI composition was calculated by dividing the integrated signal ratio of F/N of blend films by that of homopolymer PI film.

fluorine atoms. XPS measurements indicate significant segregation of PI to the surface ($\sim 100\%$), regardless of the blend ratio. The lower surface energy of PI would cause a segregation of this block to the surface. PI surface compositions greater than 100% for the blend films arise from the lower surface composition of F in the PI homopolymer film due to a surface enrichment of the dianhydride end groups without F atoms. Assuming that higher areas in AFM images in Figures 8 and 9 can be attributed a PI-rich phase with a lower surface free energy, the (40/60) blend would be expected to have a larger surface fraction of PI that is 1.89 times larger than that of the (30/70) blend film. In that case, the AFM results qualitatively correspond to the XPS

results that indicate a higher surface composition of PI for the 40/60 blend film. These results also suggest a phase separation of the P(I-*b*-AA) multiblock copolymer blend films at the surface.

Conclusion

It was shown that P(I-*b*-AA) multiblock copolymers could be prepared simply by mixing solutions of soluble PI and PAA with reactive end groups. The blend ratio strongly affects the time required to reach equilibrium, which ranges from 1 day to several weeks at 5 °C. The resultant P(I-*b*-AA) multiblock copolymers have relatively low weight-average molecular weights more than likely due to the fragmentation and redistribution of PAA component during reaction. Further, thin films of P(I-*b*-AA) multiblock copolymer exhibited surface phase separation of several tenths of microns in contrast to the micrometer-scale phase separation of the corresponding blends. The specific distribution of chemically different segments on a mesoscopic level would impart distinct properties that could be tailored. Hence, P(I-*b*-AA) can be a novel polyimide thin-film material applicable to the microelectronics.

Acknowledgment. We thank J. A. Hirsch for his help with XPS measurements. K.K. also thanks D. Howie for his help with light scattering measurements. The authors acknowledge the use of the Shared Experimental Facilities of the National Science Foundation-

supported Materials Research Science and Engineering Center (DMR98-09365).

References and Notes

- (1) Yang, C. P.; Chen, R. S.; Chen, S. H. *J. Polym. Sci., Polym. Chem.* **2001**, *39*, 93.
- (2) Tsuda, Y.; Kanegae, K.; Yasukouchi, S. *Polym. J.* **2000**, *32*, 941.
- (3) Liaw, D. J.; Liaw, B. J.; Yu, C. W. *Polymer* **2001**, *42*, 5175.
- (4) Chiniwalla, P.; Manepalli, R.; Farnsworth, K. *IEEE Trans. Adv. Pack.* **2001**, *24*, 41.
- (5) Liang, T.; Makita, Y.; Kimura, S. *Polymer* **2001**, *42*, 4867.
- (6) Hong, S.-K.; Kikuchi, H.; Kajiyama, T. *Polym. J.* **1999**, *31*, 160.
- (7) Cotts, P. M. *J. Polym. Sci., Polym. Phys.* **1986**, *24*, 923.
- (8) Swanson, S. A.; Cotts, P. M.; Siemens, R.; Kim, S. H. *Macromolecules* **1991**, *24*, 1352.
- (9) Ton-That, C.; Shard, A. G.; Teare, D. O. H.; Bradley, R. H. *Polymer* **2001**, *42*, 1121.
- (10) Tanaka, K.; Takahara, A.; Kajiyama, T. *Macromolecules* **1996**, *29*, 3232.
- (11) Lambooy, P.; Phelan, K. C.; Haugg, O.; Krausch, G. *Phys. Rev. Lett.* **1996**, *76*, 1111.
- (12) Volksen, W. *Adv. Polym. Sci.* **1994**, *117*, 111.
- (13) Sokolov, L. B. *Synthesis of Polymers by Polycondensation*. Translated by J. Schmorak, Israel Program for Scientific Translation, Jerusalem, 1968.
- (14) Odian, G. *Principles of Polymerization*, 2nd ed.; Wiley-Interscience: New York, 1981.
- (15) This topic will be submitted elsewhere.
- (16) Ree, M.; Volksen, W.; Yoon, D. Y. *J. Polym. Sci., Polym. Phys.* **1991**, *29*, 1203.

MA030002E